Study on the Photodissociation Spectra of CS_2^+ via $\tilde{B}^2\Sigma_u^+$ and $\tilde{C}^2\Sigma_g^+$ Electronic States

Xiujuan Zhuang, Limin Zhang,* Jinting Wang, Yuchao Ma, Shuqin Yu, Shilin Liu, and Xinxiao Ma

Department of Chemical Physics, University of Science and Technology of China, Hefei, Anhui 230026, China

Received: January 25, 2006; In Final Form: March 22, 2006

The photodissociation spectra of CS_2^+ ions via $\tilde{B}^2\Sigma_u^+$ and $\tilde{C}^2\Sigma_g^+$ electronic states have been studied by using two-photon excitation, where the parent CS_2^+ ions were prepared by [3 + 1] REMPI (resonance-enhanced multiphoton ionization) at 483.2 nm from the jet-cooled CS_2 molecules. The [1 + 1] photodissociation spectrum of CS_2^+ via the $\tilde{B}^2\Sigma_u^+(v_1v_20) \leftarrow \tilde{X}^2\Pi_{g,3/2}(000)$ transition was obtained by scanning the dissociation laser in the wavelength range of 270−285 nm and detecting the signal of both S^+ and CS^+. The [1 + 1′] photodissociation spectra of CS_2^+ were obtained by fixing the first dissociation laser at 281.94 or 277.15 nm to excite the $\tilde{B}^2\Sigma_u^+$ (000 or 100) ← $\tilde{X}^2\Pi_{g,3/2}(000)$ transitions and scanning the second dissociation laser in the range of 606−763 nm to excite $\tilde{C}^2\Sigma_g^+(v_1v_20) \leftarrow \tilde{B}^2\Sigma_u^+(000,100)$ transitions. New spectroscopic constants of $\nu_1 = 666.2 \pm 2.5\ cm^{-1}$, $\nu_2 = 363.2 \pm 1.9\ cm^{-1}$, $\chi_{11} = -5.5 \pm 0.1\ cm^{-1}$, $\chi_{22} = 1.6 \pm 0.1\ cm^{-1}$, $\chi_{12} = -8.6 \pm 0.2\ cm^{-1}$, and $k_{122} = 44.9 \pm 2.5\ cm^{-1}$ (Fermi resonance constant) for the $\tilde{C}^2\Sigma_g^+$ state are deduced from the [1 + 1′] photodissociation spectra. On the basis of the [1 + 1] and [1 + 1′] photodissociation spectra, the wavelength and level dependence of the product branching ratios CS^+/S^+ has been found and the dissociation dynamics of CS_2^+ ions via $\tilde{B}^2\Sigma_u^+$ and $\tilde{C}^2\Sigma_g^+$ electronic states are discussed.

I. Introduction

As an important species in astrophysics and atmospheric physics,[1] the spectroscopy and dissociation dynamics of the linear CS_2^+ ion have been studied by a variety of experimental techniques.[2−17] Optical emission from the $\tilde{A}$ and $\tilde{B}$ states of CS_2^+ was observed, and the vibrational frequencies and rotational constants were precisely determined from the spectra.[10,12] The dissociation dynamics from the electronically excited states of CS_2^+ were also studied by mass spectroscopy,[2] electron impact technique,[3] photoelectron photoion coincidence spectroscopy,[17] and photofragment excitation spectroscopy.[4−8] The $\tilde{C}$ state of CS_2^+ was found to be totally predissociative and correlated to the CS^+ and S^+ fragment ions. Eland and co-workers[2] provide an interpretation for predissociation of the $\tilde{C}$ state, beginning with internal conversion to high vibrational levels of a lower state, perhaps the $\tilde{B}$ state (through odd ν_3 vibrational coupling), that is, the vibronic coupling between two electronic states. Momigny et al.[3] presumed that the predissociations of the $\tilde{B}^2\Sigma_u^+$ and $\tilde{C}^2\Sigma_g^+$ states by the $^4\Sigma^-$ state can take place via the large spin−orbit coupling, the slower predissociaton process of the $\tilde{C}^2\Sigma_g^+$ state can be attributed to the vibronic coupling between the $\tilde{C}^2\Sigma_g^+$ and $^2\Sigma^-$ states, where $^4\Sigma^-$ and $^2\Sigma^-$ are fully repulsive states. Two-photon absorption spectroscopy with a mass-selected beam of CS_2^+ was used to study the predissociative $\tilde{C}$ state of CS_2^+ by Maier and co-workers[4,5] and recently by Hwang et al.[6] The rotationally resolved absorption spectrum of the $\tilde{C}$ state of CS_2^+ was obtained, and the predissociative lifetime of each vibrational level in $\tilde{C}$ state was determined from the line width of a single rovibrational transition.[4,5] From the product branching ratios, CS^+/S^+, for selected vibrational levels in the $\tilde{C}$ state and the average kinetic energy releases in the CS^+ and S^+ production channels measured from time-of-flight mass spectra, Hwang et al.[6] concluded that the excitation of the bending vibration enhances the CS^+ production channels more than the S^+ channel. Zhang et al.[7,8] investigated the dissociation mechanism of CS_2^+ at the energy position below the $\tilde{C}^2\Sigma_g^+$ state by using the [1 + 1] photofragment excitation (PHOFEX) spectrum of CS_2^+ and proposed that the photodissociation of CS_2^+ correlated with the $S^+(^4S) + CS(X^1\Sigma^+)$ and $CS^+(X^2\Sigma^+) + S(^3P)$ is preliminarily attributed to the $CS_2^+(\tilde{B}^2\Sigma_u^+) \leftarrow CS_2^+(\tilde{A}^2\Pi_u, \tilde{X}^+) \leftarrow CS_2^+(\tilde{X}^2\Pi_g)$ transitions and the spin−orbit coupling between the $\tilde{B}^2\Sigma_u^+$ and $^4\Sigma^-$ states.

Despite extensive studies of the spectroscopy and dissociation dynamics regarding the excited states of CS_2^+, there have been very few reports about the photodissociation spectroscopy for the $\tilde{B}^2\Sigma_u^+(v_1v_2v_3) \leftarrow \tilde{X}^2\Pi_{g,3/2}$ transition and for the transition to the $\tilde{C}^2\Sigma_g^+$ state from the vibrationally excited $\tilde{B}^2\Sigma_u^+$ state of CS_2^+, which could also provide useful information for the photochemistry of CS_2^+. On the basis of previous data[4−8] about the double resonance spectroscopy on CS_2^+, this work aims to investigate the spectrum and the predissociation dynamics of $CS_2^+(\tilde{C}^2\Sigma_g^+)$ excited from the vibrationally excited intermediate $\tilde{B}^2\Sigma_u^+$ state and to learn the wavelength and level dependence of the product branching ratios CS^+/S^+ in photodissociation. The relevant energy levels are drawn schematically in Figure 1.

II. Experimental Section

The experimental setup has been reported previously.[7] Briefly, it consists of (i) a pulsed molecular beam source to generate the jet-cooled CS_2 molecules, (ii) three dye laser systems pumped by two YAG lasers, each with a pulse width of ∼5 ns, and (iii) a homemade time-of-flight (TOF) mass spectrometer.

The jet-cooled CS_2 molecules were produced by the supersonic expansion of a CS_2/argon gas mixture (10%) through a

* To whom correspondence should be addressed. E-mail: lmzha@ustc.edu.cn.

10.1021/jp060533f CCC: $33.50
Published on Web 04/22/2006

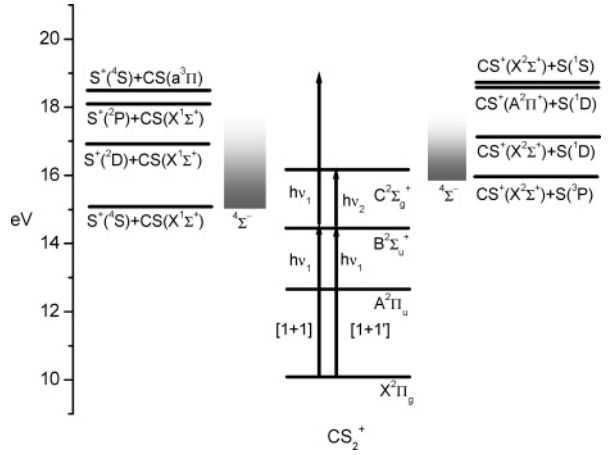

Figure 1. Schematic energy level diagram of CS_2^+ and their dissociation products, CS^+ and S^+, taken from refs 2, 3, 8, and 14. The relevant [1 + 1] and [1 + 1′] excitation processes of CS_2^+ were shown, respectively. The energy scale was based on the ground state of CS_2.

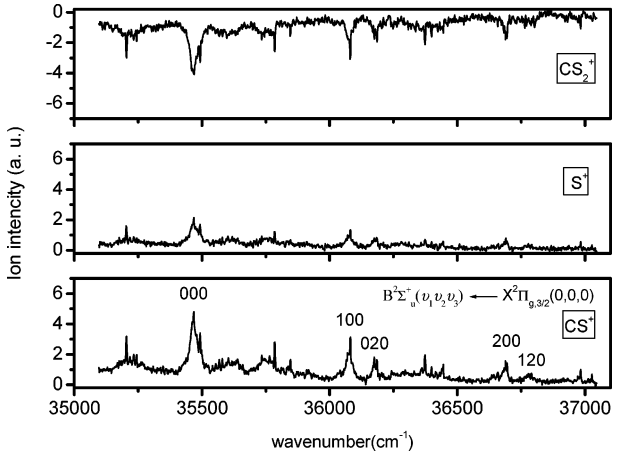

Figure 2. Photodissociation spectrum (the depletion spectrum of parent CS_2^+ ions and the enhanced spectrum of fragment ions S^+ and CS^+) obtained by scanning the dissociation laser in the range of 270−285 nm. The spectrum was assigned to the $\tilde{B}^2\Sigma_u^+(\upsilon_1\upsilon_2 0) \leftarrow \tilde{X}^2\Pi_{g,3/2}(000)$ transitions of CS_2^+.

pulsed nozzle (General Valve), with a orifice diameter of 0.5 mm, into a vacuum chamber. The laser−molecule interaction region was located 6 cm downstream from the nozzle orifice. The TOF mass spectrometer was pumped by two turbomolecular pumps with flow rates of 500 and 450 L/s, respectively. The stagnation pressure was kept at ∼3 atm, and the operating pressure in the interaction region was 2×10^{-5} Torr.

One dye laser (Lambda Physics, FL3002), that was pumped by the THG (354.7 nm) output of a Nd:YAG laser, was used for photoionization. The output of the ionization dye laser (483.2 nm, ∼1.5 mJ/pulse) was focused perpendicularly to the molecular beam of CS_2 by a quartz lens with $f = 150$ mm and was used to prepare CS_2^+ ions via [3 + 1] REMPI (resonance-enhanced multiphoton ionization) of CS_2 molecules.[9] An additional two dye lasers, pumped separately by another Nd:YAG laser (Spectra-Physics, GCR 170), were used to dissociate the prepared CS_2^+ ions. The first dissociation dye laser (270−285 nm, ∼0.02 mJ/pulse) was coaxially counterpropagated with the ionization laser and weakly focused by another quartz lens of $f = 300$ mm. The second dissociation dye laser (606−765 nm, 2−6 mJ/pulse) was coaxially propagated with the ionization laser and was focused by the same lens ($f = 150$ mm). Three or two dye lasers were temporally and spatially matched with each other at the laser−molecular interaction point. The wavelengths of the lasers were calibrated with a neon hollow cathode lamp.

The produced ions, including the parent CS_2^+ ions and the fragment ions, were extracted and accelerated in a TOF mass spectrometer, drifted along a 70 cm long TOF tube, and were finally detected by a microchannel plate (MCP). The signals from the MCP output were amplified with a preamplifier (Stanford SR240A), the signals for selected mass species were averaged with boxcar averagers (Stanford Model SR250), and then interfaced to a personal computer (PC) for data storage. The intensities of the ionization laser and the dissociation lasers were monitored simultaneously during the experiment.

III. Results and Discussion

A. [1 + 1] Photodissociation Spectrum of CS_2^+ via $\tilde{B}^2\Sigma_u^+ \leftarrow \tilde{X}^2\Pi_{g,3/2}$ Transition.[18] We prepared exclusive CS_2^+ ions in the $\tilde{X}^2\Pi_g$ state with a minimum amount of S^+ and CS^+ ions,[7] by using a lens of $f = 150$ mm to focus the ionization laser at $\lambda = 483.2$ nm and optimizing the laser pulse energy at ∼1.5 mJ. The soft ionization at this wavelength comes from the [3 + 1] REMPI of CS_2 [9]

$$CS_2(\tilde{X}^1\Sigma_g^+) \xrightarrow{3h\nu} CS_2(4p\,\sigma\,^3\Pi_u) \xrightarrow{h\nu} CS_2^+(\tilde{X}^2\Pi_g) + e \quad (1)$$

With CS_2^+ as the main ion product in the [3 + 1] REMPI of CS_2, the photodissociation spectrum of CS_2^+ ions (the depletion spectrum of parent ions and the enhanced spectrum of fragment ions) could be investigated by introducing one or two dissociation lasers.

By controlling the dissociation laser at about 0.02 mJ/pulse and scanning the laser wavelength in the range of 270−285 nm, remarkable CS^+ and S^+ signals originating from the dissociation of the parent CS_2^+ ions could be observed in the TOF mass spectrum. Figure 2 shows the depletion spectrum of parent CS_2^+ ions and the enhancement spectrum of fragment CS^+ and S^+ ions obtained by monitoring CS_2^+, CS^+, and S^+, respectively. With the aid of the spectroscopic data in previous studies,[10−14] this photodissociation spectrum could be assigned as the electronic transition $\tilde{B}^2\Sigma_u^+(\upsilon_1\upsilon_2 0) \leftarrow \tilde{X}^2\Pi_{g,3/2}(000)$ of CS_2^+, where υ_1 and υ_2 represent the vibrational quantum numbers of the ν_1 and ν_2 modes, respectively. The assignments of the photodissociation spectrum are given in Figure 2 and listed in Table 1. Also listed in Table 1 are the spectral data deduced from the emission spectrum[12] and the photoionization spectrum.[13] Although the photoexcitation of the $\tilde{B}^2\Sigma_u^+(000) \leftarrow \tilde{X}^2\Pi_{g,3/2}(000)$ transition was used in previous studies,[4−6] the report about the photoexcitation spectrum of the $\tilde{B}^2\Sigma_u^+(\upsilon_1\upsilon_2 0) \leftarrow \tilde{X}^2\Pi_{g,3/2}(000)$ transition has gone largely unnoticed until now. Since the vibrational frequencies of CS_2^+ have the approxima-

TABLE 1: Wavenumbers and Vibrational Assignments for the Observed $\tilde{B}^2\Sigma_u^+(\upsilon_1\upsilon_2 0) \leftarrow \tilde{X}^2\Pi_{g,3/2}(000)$ Spectrum in the [1 + 1] Photodissociation of CS_2^+

$\leftarrow \tilde{X}^2\Pi_{g,3/2}(000)$ $\tilde{B}^2\Sigma_u^+(\upsilon_1\upsilon_2 0)$	ν_{exp} (cm^{-1})	refs 4 and 5	ref 12[a]	ref 13[b]	spacing (cm^{-1})
000	35 468	35 460	35 461	35 507	0
100	36 081		36 063	36 110	613
020	36 175				707
200	36 690				1222
120	36 783				1315

[a] Values taken from the electronic emission spectrum in ref 12. [b] Values deduced from the photoionization resonance spectrum of CS_2 in ref 13.

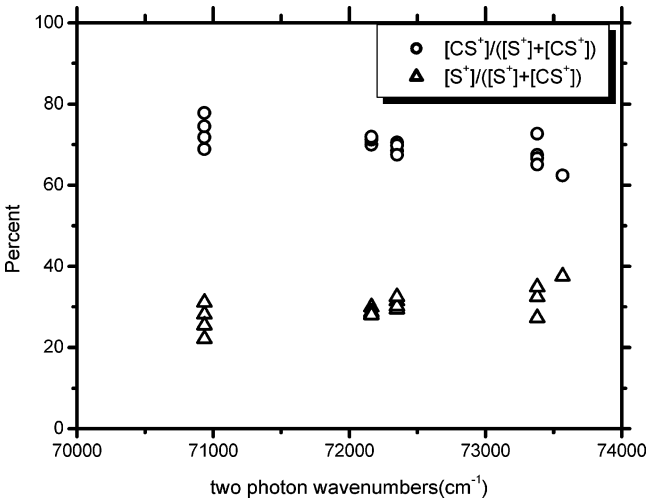

Figure 3. Percentage branching to each product ion in the [1 + 1] excitation and photodissociation processes via the $\tilde{B}^2\Sigma_u^+(v_1v_20) \leftarrow \tilde{X}^2\Pi_{g,3/2}(000)$ transitions of CS_2^+.

tion $\nu_1 \sim 2\nu_2$, Fermi resonance interaction is expected to occur between the (v_1,v_2,v_3) and (v_1-1,v_2+2,v_3) vibrational levels. Two Fermi resonance pairs of the $\tilde{B}^2\Sigma_u^+$ state with $(2v_1 + v_2) = 2, 4$ are observed, as shown in Figure 2. Since the Fermi resonance will shift the zero-order vibrational energy levels, the exact values of ν_1 and ν_2 cannot be obtained simply from the frequency intervals in Table 1. In the case of only a few spectral peaks available, however, the vibrational frequencies may approximately be inferred as $\nu_1 = 613$ cm^{-1} and $2\nu_2 = 707$ cm^{-1} for the $\tilde{B}^2\Sigma_u^+$ state by ignoring the modes mixing and anharmonicity. Moreover, in Figure 2, no spectrum related to the transition from $CS_2^+(\tilde{X}^2\Pi_{g,1/2})$ could be found; this fact can be explained, at least, by the strong population of $\tilde{X}^2\Pi_{g,3/2}(0,0,0)$ and the weak population of $\tilde{X}^2\Pi_{g,1/2}(0,0,0)$ in the [3 + 1] REMPI process of the CS_2 at 483.2 nm.[15]

Because the energy levels of $\tilde{B}^2\Sigma_u^+$ related to the resonance peaks in Figure 2 are all less than the first dissociation limit (4.6 eV) to produce S^+ and the second dissociation limit (5.852 eV) to produce CS^+,[2,3,8,16,17] two photons are needed to dissociate $CS_2^+(\tilde{X}^2\Pi_{g,1/2})$. It means that the dissociation process via the $\tilde{B}^2\Sigma_u^+ \leftarrow \tilde{X}^2\Pi_{g,3/2}$ transition of CS_2^+ to produce CS^+ and S^+ is a [1 + 1] process. Another piece of evidence supporting the presumption of the [1 + 1] dissociation mechanism is the branching ratios CS^+/S^+ measured in this work. Figure 3 shows the CS^+/S^+ branching ratios obtained from Figure 1 at two-photon energy. The product branching ratios CS^+/S^+ of 2−4, in the energy range (8.7−9.2 eV) reached by a two-photon excitation of CS_2^+, agree well with that given by the photoelectron photoion coincidence spectroscopy of CS_2.[17] Although the two-photon energy (8.7−9.2 eV) of a dissociation laser in the 270−285 nm range is above several dissociation limits of CS_2^+ and the threshold to produce S^+ is lower than CS^+, as shown in Figure 1, the excess of CS^+ over S^+ in Figures 2 and 3 indicates that the lowest energy channel is not favored.[17] On the other hand, the TOF profiles of the fragment ions (CS^+, S^+) do not show evident broadening comparing with that of the parent ions (CS_2^+), indicating that the released kinetic energy of fragment ions in the [1 + 1] dissociation process of CS_2^+ is limited and the products may be in the excited states. All of these facts could be explained reasonably as follows: in this energy range there are the repulsive surfaces connecting each set of products to the manifold of states with high density, thus a viable curve crossing will always be available at an outer turning point of potential curve, and the kinetic energy releases

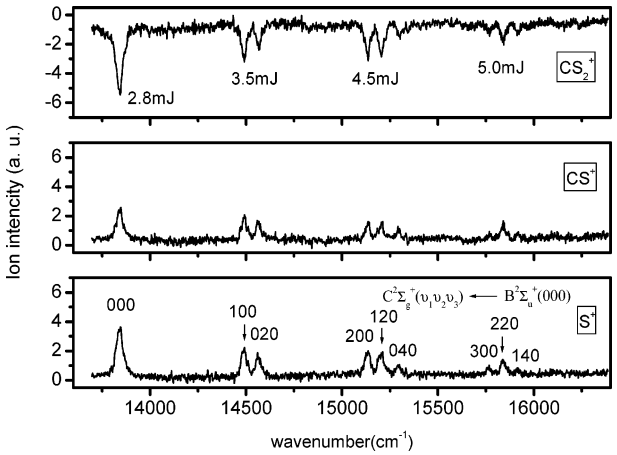

Figure 4. Photodissociation spectrum obtained by fixing the first dissociation laser at 281.94 nm and scanning the second dissociation laser in the range of 650−730 nm. The spectrum was assigned to the $\tilde{C}^2\Sigma_g^+(v_1v_20) \leftarrow \tilde{B}^2\Sigma_u^+(000)$ transitions of CS_2^+. The energy per pulse of the second dissociation laser was marked at the position of the resonance peaks in the upper figure.

will be limited by the limited steepness of repulsive surfaces at extended internuclear distances.[17]

To check if there is any disturbance from the ionization laser on the photodissociation of CS_2^+, we repeated the experiment with about a 60 ns delay and a slight separation in the direction of ion flight between the dissociation laser and the ionization laser in the laser−molecule interaction region. The ∼60 ns delay means that there is no temporal overlap between the ionization laser and the dissociation laser, when using roughly a 5 ns laser pulse width. This result is consistent with those obtained with no delay. Hence, the disturbance from the ionization laser can be negligible in the photodissociation experiment of CS_2^+. The [1 + 1] photodissociation process of CS_2^+ via the $\tilde{B}^2\Sigma_u^+ \leftarrow \tilde{X}^2\Pi_{g,3/2}$ transition can be expressed as the following

$$CS_2^+(\tilde{X}^2\Pi_g) \xrightarrow{h\nu} CS_2^+(\tilde{B}^2\Sigma_u^+)$$

$$CS_2^+(\tilde{B}^2\Sigma_u^+) \xrightarrow{h\nu} CS_2^+ \text{ (higher state within 8.7−9.2 eV)}$$

$$CS_2^+ \text{ (higher state within 8.7−9.2 eV)} \rightarrow CS + S^+$$

$$\rightarrow CS^+ + S$$

B. [1 + 1′] Photodissociation Spectra of CS_2^+ via $\tilde{C}^2\Sigma_g^+ \leftarrow \tilde{B}^2\Sigma_u^+$(000, 100) Transitions. Fixing the first dissociation laser at 281.94 or 277.15 nm to excite the $\tilde{B}^2\Sigma_u^+$(000 or 100) $\leftarrow \tilde{X}^2\Pi_g(000)$ transition of CS_2^+, the CS^+ and S^+ signals will be seen in the TOF mass spectrum as mentioned in section A. Regarding the CS^+ and S^+ signals produced by the first dissociation laser as a background and scanning the second dissociation laser in the range of 606−765 nm to excite the $\tilde{C}^2\Sigma_g^+ \leftarrow \tilde{B}^2\Sigma_u^+$ (000 or 100) transitions of CS_2^+, a decreasing of CS_2^+ signals and an increasing of the CS^+ and S^+ signals were observed. In this way, the [1 + 1′] photodissociation spectrum was obtained, as shown in Figures 4 and 5. With the aid of the spectroscopic data obtained from previous studies on the spectroscopy of CS_2^+,[4−6,13,14] these photodissociation spectra could be assigned completely as the electronic transition $\tilde{C}^2\Sigma_g^+(v_1v_20) \leftarrow \tilde{B}^2\Sigma_u^+$(000 or 100) of CS_2^+. The assignments for the photodissociation spectra were given in Figures 4 and 5 and in Table 2. The 10 vibrational bands of the $\tilde{C}(v_1v_20) \leftarrow \tilde{B}(100)$ transitions are observed for the first time. The energy per pulse

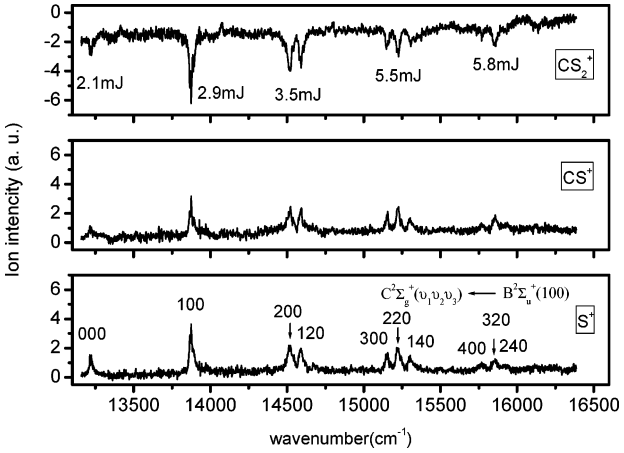

Figure 5. Photodissociation spectrum obtained by fixing the first dissociation laser at 277.15 nm and scanning the second dissociation laser in the range of 606−763 nm. The spectrum was assigned to the $\tilde{C}^2\Sigma_g^+(v_1v_20) \leftarrow \tilde{B}^2\Sigma_u^+(100)$ transition of CS_2^+. The energy per pulse of the second dissociation laser was marked at the position of the resonance peaks in the upper figure.

of the second dissociation laser is marked at the position of the resonance peaks.

With the approximation $\nu_1 \sim 2\nu_2$ for $CS_2^+(\tilde{C}^2\Sigma_g^+)$, Fermi resonance interaction is expected to occur between the (v_1,v_2,v_3) and (v_1-1,v_2+2,v_3) vibrational levels. The vibrational term values for $CS_2^+(\tilde{C}^2\Sigma_g^+)$ can be written as

$$\langle u_1,v_2,v_3|H|v_1,v_2,v_3\rangle = G(v_1,v_2,v_3) = \sum_i \nu_i\left(v_i+\frac{d_i}{2}\right)+\sum_{i\le j}\chi_{ij}\left(v_i+\frac{d_i}{2}\right)\left(v_j+\frac{d_j}{2}\right) \quad (1)$$

where **H** refers to the Hamiltonian and χ_{ij} and d_i are the anharmonic constant and the degeneracy of vibrational levels, respectively, of the $\tilde{C}^2\Sigma_g^+$ state. The Fermi resonance interaction is related to the off-diagonal terms for each $(2v_1 + v_2)$ block[19]

$$\langle v_1,v_2,v_3|H|v_1-1,v_2+2,v_3\rangle = -\frac{k_{122}}{4}\sqrt{v_1}\,(v_2+2) \quad (2)$$

where k_{122} is the constant of Fermi resonance interaction between the ν_1 and ν_2 modes.

By diagonalizing the effective Hamilton matrix and fitting the identified $\tilde{C}^2\Sigma_g^+$ $(v_1v_20) \leftarrow \tilde{B}^2\Sigma_u^+$ (000,100) peaks with a least-squares procedure, the spectral constants of the $\tilde{C}^2\Sigma_g^+$ state can be determined. New spectral constants of $\nu_1 = 666.2 \pm 2.5$ cm^{-1}, $\nu_2 = 363.2 \pm 1.9$ cm^{-1}, $\chi_{11} = -5.5 \pm 0.1$ cm^{-1}, $\chi_{22} = 1.6 \pm 0.1$ cm^{-1}, $\chi_{12} = -8.6 \pm 0.2$ cm^{-1}, and $k_{122} = 44.9 \pm 2.5$ for the $\tilde{C}^2\Sigma_g^+$ state were fitted out from all the $\tilde{C}^2\Sigma_g^+(v_1v_20)$ $\leftarrow \tilde{B}^2\Sigma_u^+$ (000,100) transitions of the [1 + 1′] photodissociation spectrum and are listed in Table 3. The term values calculated with the spectral constants in Table 3 are also listed in Table 2. As can be seen, the differences between the calculated and observed values are less than 4 cm^{-1}, which should be acceptable for the vibrationally resolved spectrum. The vibrational bandwidths of 30−40 cm^{-1} were observed, and no rotational structure can be resolved in the [1 + 1] and [1 + 1′] photodissociation spectra by finely scanning the two dissociation lasers.

TABLE 3: Spectral Constants of the $\tilde{C}^2\Sigma_g^+$ State Determined by Least-square Fitting of the $\tilde{C}^2\Sigma_g^+(v_1v_20) \leftarrow \tilde{B}^2\Sigma_u^+$(000,100) Spectrum[a]

	this work	ref 13	ref 5
ν_1	666.2 ± 2.5	651	652
ν_2	363.2 ± 1.9		364
χ_{11}	−5.5 ± 0.1		
χ_{22}	1.6 ± 0.1		
χ_{12}	−8.6 ± 0.2		
k_{122}	44.9 ± 2.5		
T_0	49310 ± 5[b]	49 325	49 352

[a] All values are in units of cm^{-1}. [b] Value calculated by adding the wavenumbers of $\tilde{B}^2\Sigma_u^+(000) \leftarrow \tilde{X}^2\Pi_{g,3/2}(000)$ transition.

The first dissociation limit $S^+(^4S) + CS(X^1\Sigma^+)$ and the second dissociation limit $CS^+(X^2\Sigma^+) + S(^3P)$ of CS_2^+ locate at 4.6 and 5.85 eV above $CS_2^+(\tilde{X}^2\Pi_{g,3/2}(000))$, respectively.[2,3,8,16,17] By fixing the first dissociation laser at 281.94 or 277.15 nm (4.40 or 4.47 eV) and scanning the second dissociation laser at 765−606 nm (1.62−2.05 eV), the two-photon energy of 6.02−6.52 eV in the [1 + 1′] excitation process will be higher than the first and second dissociation limits as shown in Figure 1. Hence, the [1 + 1′] dissociation of CS_2^+ correlated with the first and second dissociation limits could be explained by the predissociation of the $\tilde{C}^2\Sigma_g^+$ state. The dissociation of the $\tilde{C}^2\Sigma_g^+$ state may be related to complicated processes as mentioned in section I. For example, it is possible that the predissociation of the $\tilde{C}$ state begins with internal conversion to high vibrational levels of the $\tilde{B}$ state (through odd ν_3 vibrational coupling) as proposed by Eland and co-workers.[2] However, the dissociation of the $\tilde{C}^2\Sigma_g^+$ state should finally proceed via the coupling between the $\tilde{C}^2\Sigma_g^+$ state and the repulsive states correlated with the limits of $S^+(^4S) + CS(X^1\Sigma^+)$ and $CS^+(X^2\Sigma^+) + S(^3P)$. Because the spin quantum number S > 0 for the $\tilde{C}^2\Sigma_g^+$ state and for the repulsive $^4\Sigma^-$ state, large spin−orbit interactions[20] will exist between them and the dissociation of the $\tilde{C}^2\Sigma_g^+$ state can proceed via the coupling between the $\tilde{C}^2\Sigma_g^+$ state and the repulsive $^4\Sigma^-$ state. Owing to the fact that the $CS(X^1\Sigma^+) + S^+(^4S)$ limit (4.6 eV) is 1.25 eV lower than the $CS^+(X^2\Sigma^+) + S(^3P)$ limit (5.85 eV), the S^+ ions should obtain more kinetic energy than CS^+ ions and the width of the TOF mass spectral

TABLE 2: Wavenumbers and Vibrational Assignments for the Observed $\tilde{C}^2\Sigma_g^+$ $(v_1v_20) \leftarrow \tilde{B}^2\Sigma_u^+(v_100)$ Spectrum in the [1 + 1′] Photodissociation of CS_2^+

$\tilde{C}(v_1v_20)$ $\leftarrow \tilde{B}(000)$	ν_{exp}/ cm^{-1}	ν_{cal}/ cm^{-1} [a]	$(\nu_{exp}-\nu_{cal})$/ cm^{-1}	$\tilde{C}(v_1v_20)$ $\leftarrow \tilde{B}(100)$[b]	ν_{exp}/ cm^{-1}	ν_{cal}/ cm^{-1}	$(\nu_{exp}-\nu_{cal})$/ cm^{-1}
000	13 842	13 841	1	000	13 221	13 223	−2
100	14 491	14 493	−2	100	13 875	13 875	0
020	14 569	14 565	4	200	14 518	14 517	1
200	15 138	15 135	3	120	14 590	14 590	0
120	15 206	15 208	−2	300	15 152	15 150	2
040	15 301	15 302	−1	220	15 223	15 225	−2
300	15 769	15 768	1	140	15 300	152 300	−0
220	15 841	15 843	−2	400	15 772	15 774	−2
140	15 917	15 918	−1	320	15 855	15 853	2
				240	15 935	15 933	2

[a] Values calculated by using the spectral constants given in Table 3. [b] New excitation spectrum observed in this work.

peaks of the S^+ ions should be larger than that of the CS^+ ions, as observed by Hwang et al.[6] and by us in this work.

To investigate the dependence of the predissociation of CS_2^+-($\tilde{C}^2\Sigma_g^+$) on the vibrational levels of the intermediate $\tilde{B}^2\Sigma_u^+$ state, we compared the intensity distributions of spectral peaks and the product branching ratios CS^+/S^+ of $\tilde{C}(v_1v_20) \leftarrow \tilde{B}(100)$ transitions with that of $\tilde{C}(v_1v_20) \leftarrow \tilde{B}(000)$ transitions in the [1 + 1′] photodissociation spectrum. As shown in Figures 4 and 5, the (020) vibration bands of the $\tilde{C}^2\Sigma_g^+$ state appearing in the spectrum of $\tilde{C}(v_1v_20) \leftarrow \tilde{B}(000)$ transitions do not appear in the spectrum of $\tilde{C}(v_1v_20) \leftarrow \tilde{B}(100)$ transitions. This fact, which may originate from the much smaller Franck−Condon factor of the $\tilde{C}^2\Sigma_g^+(020) \leftarrow \tilde{B}^2\Sigma_u^+(100)$ transition, shows that the predissociation path of $CS_2^+(\tilde{C}^2\Sigma_g^+)$ in the [1 + 1′] process is indeed affected by the vibrational levels of the intermediate $\tilde{B}^2\Sigma_u^+$ state.

Another interesting feature shown in Figures 4 and 5 is the decreasing of the peaks corresponding to the $\tilde{C}(v_100)$ and the increasing of the peaks corresponding to the $\tilde{C}(v_1-1,2,0)$ with increasing v_1. Owing to the Fermi resonance interaction between the (v_1,v_2,v_3) and (v_1-1,v_2+2,v_3) vibrational levels, the weak $\tilde{C}^2\Sigma_g^+(v_120) \leftarrow \tilde{B}^2\Sigma_u^+$(000 or 100) transition can become strong by borrowing intensity from the strong $\tilde{C}^2\Sigma_g^+((v_1+1)00) \leftarrow \tilde{B}^2\Sigma_u^+$(000 or 100) transition. In addition, the dissociation of the $\tilde{C}^2\Sigma_g^+$ state is also affected by the dissociation rate of $\tilde{C}^2\Sigma_g^+$-(v_1v_20). Although further study is needed to determine which affects mainly the decreasing of the peaks corresponding to the $\tilde{C}(v_100)$ and the increasing of the peaks corresponding to the $\tilde{C}(v_1-1,2,0)$ with increasing v_1, it is worth to point out that a similar feature does not appear in the [1 + 1] photodissociation spectrum via the $\tilde{B}^2\Sigma_u^+(v_1v_20) \leftarrow \tilde{X}^2\Pi_{g,3/2}(000)$ transition of CS_2^+, as shown in Figure 2, but was observed in the laser-induced fluorescence (LIF) spectrum of the electronic transition $\tilde{A}^2\Pi_{u,3/2}$ $(v_1v_20) \leftarrow \tilde{X}^2\Pi_{g,3/2}(000)$ of CS_2^+.[21] Hence, the decrease of the peaks corresponding to the $\tilde{C}(v_100)$ and the increase of the peaks corresponding to the $\tilde{C}(v_1-1,2,0)$ with increasing v_1 could be, mainly or partly, attributed to the Fermi interaction between the (v_1,v_2,v_3) and (v_1-1,v_2+2,v_3) vibrational levels of the $\tilde{C}^2\Sigma_g^+$ state.

On the other hand, the branching ratios CS^+/S^+ of ∼1 for the $\tilde{C}^2\Sigma_g^+(v_1v_20) \leftarrow \tilde{B}^2\Sigma_u^+$(000 or 100) transition, as shown in Figures 4 and 5, are consistent with that of the photoelectron−photoion coincidence spectroscopy[17] and that of the optical−optical double resonance technique[6] within the same energy region but differ obviously from that of 2−4 for the [1 + 1] photodissociation process via the $\tilde{B}^2\Sigma_u^+(v_1v_20) \leftarrow \tilde{X}^2\Pi_{g,3/2}(000)$ transition of CS_2^+ within the different energy region. It means that the [1 + 1] and [1 + 1′] dissociation paths of CS_2^+ can be, at least, identified by the CS^+/S^+ branching ratios, and it provides the possibility to select the photodissociation products of the CS_2^+ ion by choosing the excitation wavelength.

The [1 + 1′] predissociation process of CS_2^+ to produce CS^+ and S^+ can be expressed as follows.

$$CS_2^+(\tilde{X}^2\Pi_{g,3/2}) \xrightarrow{h\nu} CS_2^+(\tilde{B}^2\Sigma_u^+ (000) \text{ or } (100))$$

$$CS_2^+(\tilde{B}^2\Sigma_u^+(000) \text{ or } (100)) \xrightarrow{h\nu'} CS_2^+(\tilde{C}^2\Sigma_g^+)$$

$$CS_2^+(\tilde{C}^2\Sigma_g^+) \xleftrightarrow{\text{spin-orbit}} CS_2^+(^4\Sigma^-)$$

$$CS_2^+(^4\Sigma^-) \rightarrow CS(X^1\Sigma^+) + S^+(^4S)$$

$$CS_2^+(^4\Sigma^-) \rightarrow CS^+(X^2\Sigma^+) + S(^3P)$$

IV. Summary

The [1 + 1] and [1 + 1′] photodissociation spectra of CS_2^+ ions have been obtained by using the optical resonance method. New spectral bands of $\tilde{C}(v_1v_20) \leftarrow \tilde{B}(100)$ transitions are observed. From the [1 + 1′] photodissociation spectrum via the $\tilde{B}^2\Sigma_u^+$ and $\tilde{C}^2\Sigma_g^+$ states, new spectral constants, especially the Fermi resonance constant, for the $\tilde{C}^2\Sigma_g^+$ state have been deduced. The product branching ratios CS^+/S^+ of 2−4 in the [1 + 1] photodissociation process of CS_2^+ via the $\tilde{B}^2\Sigma_u^+ \leftarrow \tilde{X}^2\Pi_{g,3/2}$ transition is obviously more than that of ∼1 in the [1 + 1′] photodissociation spectra of CS_2^+ via $\tilde{C}^2\Sigma_g^+ \leftarrow \tilde{B}^2\Sigma_u^+ \leftarrow \tilde{X}^2\Pi_{g,3/2}$ transitions. The difference of the intensity distribution between the photodissociation spectrum of the $\tilde{C}(v_1v_20) \leftarrow \tilde{B}(100)$ transition and that of the $\tilde{C}(v_1v_20) \leftarrow \tilde{B}(000)$ transition have been found in the [1 + 1′] photodissociation process. This kind of wavelength and level dependence of branching into the alternative $S + CS^+$ and $S^+ + CS$ dissociation channels provides useful information for the state selected and vibrationally excited photochemistry of molecular ions.

Acknowledgment. This work was supported financially by the National Natural Science Foundation of China (No. 20373067) and the NKBRSF research program (No. G1999075304).

References and Notes

(1) Hudson, R. D. *Rev. Geophys. Space Phys*. **1970**, *9*, 305.
(2) Brehm, B.; Eland, J. H. D.; Frey, R.; Kustler, A. *Int. J. Mass Spectrom. Ion Phys*. **1973**, *12*, 213.
(3) Momigny, J.; Mathieu, G.; Wankenne, H. *Chem. Phys. Lett*. **1973**, *21*, 606.
(4) Danis, P. O.; Wyttenbach, T.; Maier, J. P. *J. Chem. Phys*. **1988**, *88*, 3451.
(5) Evard, D. D.; Wyttenbach, T.; Maier, J. P. *J. Phys. Chem*. **1989**, *93*, 3522.
(6) Hwang, W. G.; Kim, H. L.; Kim, M. S. *J. Chem. Phys*. **2000**, *113*, 4153.
(7) Zhang, L.; Chen, J.; Xu, H.; Dai, J.; Liu, S.; Ma, X. *J. Chem. Phys.* **2001**, *114*, 10768.
(8) Zhang, L.; Wang, F.; Wang, Z.; Yu, S.; Liu, S.; Ma, X. *J. Phys. Chem. A* **2004**, *108*, 1342.
(9) Baker, J.; Konstantaki, M.; Couris, S. *J. Chem. Phys*. **1995**, *103*, 2436.
(10) Callomon, J. H. *Proc. R. Soc. London, Ser. A* **1958**, *244*, 220.
(11) Lee, L. C.; Judge, D. L.; Ogawa, M. *Can. J. Phys*. **1975**, *53*, 1861.
(12) Balfour, W. J. *Can. J. Phys*. **1976**, *54*, 1969.
(13) Frey, R.; Gotchev, B.; Peatman, W. B.; Pollak, H.; Schlag, E. W. *Int. J. Mass Spectrom. Ion Phys*. **1978**, *26*, 137.
(14) Baltzer, P.; Wannberg, B.; Lundqvist, M.; Karlsson, L.; Holland, D. M. P.; MacDonald, M. A.; Hayes, M. A.; Tomasello, P.; von Niessen, W. *Chem. Phys*. **1996**, *202*, 185.
(15) Morgan, R. A.; Baldwin, M. A.; Orr-Ewing, A. J.; Ashfold, M. N. R.; Buma, W. J.; Milan, J. B.; Lange, C. A. de. *J. Chem. Phys*. **1996**, *104*, 6117.
(16) Shukla, A. K.; Tosh, R. E.; Chen, Y. B.; Futrell, J. H. *Int. J. Mass Spectrom. Ion Processes* **1995**, *146*, 323.
(17) Aitchison, D.; Eland, J. H. D. *Chem. Phys*. **2001**, *263*, 449.
(18) Zhuang, X.; Zhang, L.; Wang, J.; Ma, Y.; Yu, S. *Chin. J. Chem. Phys*. **2005**, *18*, 657.
(19) Bernath, P. F.; Dulick, M.; Field, R. W. *J. Mol. Spectrosc*. **1981**, *86*, 275.
(20) Herzberg, G. *Molecular spectra and molecular structure. III. Electronic spectra and electronic structure of polyatomic molecules*; Van Nostrand: Princeton, NJ, 1966; p 460.
(21) Bondybey, V. E.; English, J. H.; Miller, T. A. *J. Chem. Phys*. **1979**, *70*, 1621.